Journal of ELECTRONIC MATERIALS
DOI: 10.1007/s11664-015-4122-9

Phase Content and Thermoelectric Properties of Optimized Thermoelectric Structures Based on the Ag-Pb-Sb-Te System

IHOR HORICHOK,[1] RASIT AHISKA,[2] DMYTRO FREIK,[1] LYUBOMYR NYKYRUY,[1,4] STEPAN MUDRY,[3] OSTAP MATKIVSKIY,[1] and TARAS SEMKO[1]

1.—Vasyl Stefanyk Precarpathian National University, Shevchenko Str. 57, Ivano-Frankivsk 76018, Ukraine. 2.—Gazi University, Teknikokullar, 06500 Ankara, Turkey. 3.—Ivan Franko National University of Lviv, Universytetska St. 1, Lviv 79000, Ukraine. 4.—e-mail: lyubomyr.nykyruy@gmail.com

Results of x-ray studies and measurements of thermoelectric parameters (Seebeck coefficient S, specific electrical conductivity σ, and thermal conductivity χ) of materials based on lead telluride, such as PbTe, PbTe:Sb, PbTe-Sb_2Te_3, $Pb_{18}Ag_1Sb_1Te_{20}$, $Pb_{18}Ag_2Te_{20}$, and PbTe-Ag_2Te, are presented. It was found that PbTe:Sb (with 0.3 at.% Sb) as well as $Pb_{18}Ag_1Sb_1Te_{20}$ and $Pb_{18}Ag_2Te_{20}$ systems have the highest thermoelectric figure of merit values. In the case of PbTe:Sb, this is due to a significant increase of the electrical conductivity. In the cases of $Pb_{18}Ag_1Sb_1Te_{20}$ and $Pb_{18}Ag_2Te_{20}$, it is due to an increase of the Seebeck coefficient and a significant reduction in the thermal conductivity compared with pure PbTe.

Key words: Lead telluride, doping, solid solutions, LAST, thermoelectric properties

INTRODUCTION

Development of new energy-saving technologies and creation of effective renewable energy sources, waste heat utilization, and development of autonomous energy sources are the highest-priority areas of modern research. The utmost importance of these topics is due to fossil-fuel limits and significant emissions of greenhouse gases into the atmosphere that lead to global climate changes. Therefore, research on direct conversion of heat into electricity is at the cutting edge of modern science. Thermoelectric (TE) converters are among the most reliable sources of electricity, allowing continuous operation for decades.[1–6] They play an important role in advancing global sustainable energy solutions.

The efficiency of a thermoelectric material is determined by the dimensionless thermoelectric figure of merit (ZT),

$$ZT = \left(\frac{S^2\sigma}{\chi}\right)T, \quad (1)$$

where S, σ, χ, and T are the Seebeck coefficient, specific electrical conductivity, thermal conductivity, and the absolute temperature, respectively.[1–6] The value of ZT is approximately 0.5 to 1.0 for the most popular materials used in modern thermoelectric generators.[1,2,7] Increasing this parameter to values of approximately 1.5 to 2.0 would significantly expand the use of TE converters. The main obstacle is the interdependence of S, σ, and χ, which does not allow improvement of one of these parameters without compromising another.[6]

The main way of obtaining materials with high values of ZT is to search for new materials or modify the properties of already known ones. Moreover, the latter method has several advantages. In particular, one can use technology already developed for the basic material.

It should be noted that lead telluride (PbTe) is a famous thermoelectric material used in production of electrical power generators. ZT values of 0.7 to 0.8 are accepted for nondoped material.[5,6] However,

(Received June 2, 2015; accepted October 5, 2015)

Published online: 27 October 2015

its main parameters can be effectively changed by doping and creating solid solutions.[8–14] Doping with antimony is especially promising.[10–13] In the valence shell, antimony (Sb) has one more electron compared with Pb. On replacement of lead ions by antimony, the extra electron goes into the conduction band, causing an increase of the free carrier concentration and leading to n-type conductivity.

In the case of PbTe-Sb_2Te_3 solid solutions, the thermoelectric properties can be further improved by reducing the thermal conductivity due to enhancement of the effective phonon scattering at point defects of the crystal lattice.[14]

In recent years, a significant increase of the efficiency of thermoelectric materials based on lead telluride has been achieved through the creation of the new class of compounds $Ag_xPb_mSb_{2-x}Te_{m+2}$ (LAST).[15–19] The atoms of silver (acceptor) and antimony (donor) occupy positions in the cation sublattice of these materials and compensate the electric effect of each other without substantially impacting on the electronic subsystem. However, emerging nanoscale violations of the crystalline lattice in Ag- and Sb-enriched areas[15] effectively scatter phonons, leading to a significant decrease of the thermal conductivity. Thus, the thermoelectric properties strongly depend on the values m and x, and on the conditions of material production.[19]

As a result of research on the $Ag_xPb_mSb_{2-x}Te_{m+2}$ system conducted by the authors,[15] it was found that the most suitable value of m is 18. By varying the ratio of Ag to Sb, one can effectively change the conductivity and Seebeck coefficient of the material,[20,21] as well as the shape and chemical composition of the precipitates formed.[22–25] It should be noted that, as shown in Ref. 24, the ratio of antimony to silver atoms in the matrix and in the different precipitates essentially depends on the technological conditions during material production, including its annealing.

Structural, energy, and thermodynamic parameters of the Pb-Ag-Sb-Te system for different chemical compositions calculated from first principles are presented in Refs. 26–29. It was found that isolated atoms of silver create resonance acceptor states in the valence band, whereas atoms of antimony create donor states in the conduction band. At the same time, the simultaneous presence of Ag and Sb in the crystal lattice leads to changes in the energy structure, which, in addition to the chemical composition, shows strong sensitivity to the spatial configuration and symmetry of atoms.

The temperature-dependent mechanical properties (microhardness, Young's modulus, and Poisson's ratio) of LAST compounds for different chemical compositions and sample preparation conditions were investigated in Refs. 30, 31.

High values of the dimensionless thermoelectric figure of merit have been achieved in the PbTe-Ag_2Te system by additional strong doping with Na (La) to obtain p-type (n-type) conductivity.[32] For our specific conditions of material synthesis and cooling, Ag_2Te formed nanoscale precipitates that effectively scattered phonons, reducing the thermal conductivity of the material. Thus, admixture of sodium or lanthanum improved the conductivity and Seebeck coefficient values.

The problem of selecting an effective alloying component, its concentration, and the significant dependence of the material properties on the conditions of sample preparation are important in materials science today. Therefore, this paper presents comparative analysis of the influence of promising alloying components on the properties of thermoelectric samples based on PbTe, obtained by cold pressing followed by annealing.

The choice of technology was determined by several factors. First, pressed samples are characterized by much better mechanical properties compared with those cut from polycrystalline ingot samples.[22] Second, the proper choice of the cold-pressing mode leads to high-quality samples. Their properties are not significantly worse compared with samples obtained by hot pressing.[33] Also, the lower energy consumption during production provides greater competitiveness of such samples.

EXPERIMENTAL PROCEDURES

Synthesis of materials was carried out in quartz ampoules evacuated to residual pressure of 10^{-4} Pa. The ampoules were subjected to detailed purification, which included the following steps: washing in a mixture of HNO_3:H_2SO_4:H_2O, washing with distilled water, washing with 30% hydrogen peroxide to clean residual acids, frequent washing with distilled water, steaming in bidistillate vapor, and oven-drying at T = 420 K to 470 K.

Raw materials (metals, chalcogen) of 99.99% purity were subjected to additional purification for the following synthesis. Evacuated ampoules containing mixtures of the components were placed in an electric oven that can vary the angle in the range of ±30° from horizontal with a period of 300 s to force mixing of the components. The numerical values of the synthesis temperature were defined from the state diagrams. Cooling was performed at the rate of 5 K/h to temperature of 600 K to 700 K. In future experiments, cooling will be performed at the rate of 10 K/h.

The obtained ingots were ground in an agate mortar and compressed under pressure of 1.5 GPa to 2.5 GPa after selecting the fraction of size 0.05 mm to 0.5 mm. The resulting cylindrical samples were subjected to annealing in air at 400 K to 700 K during 18,000 s to 72,000 s. To measure the Seebeck coefficient and specific electrical conductivity, d = 5 mm and $l \approx 8$ mm size samples were used, whereas for measuring the thermal conductivity coefficient, d = 8 mm and $l \approx 12$ mm size samples were used.

The phase composition and structure of the synthesized ingots and pressed samples were examined using x-ray methods on an automatic diffractometer (STOE STADI P; STOE & Cie GmbH, Germany) with a linear position-sensitive detector according to the Gigner modified geometry scheme. Calculation of theoretical diffractions for known compounds for phase identification and determination of unit cell parameters was performed with STOE WinXPOW (version 3.03) and PowderCell (version 2.4) software packages. Refinement of crystal structure phase for select samples in the isotropic approximation for atomic displacement parameters was conducted by the Rietveld method using pseudo-Voigt profile functions with the help of FullProf.2k (version 5.30) from the WinPLOTR software package. Possible prevailing orientation (texture) of main phase grains was determined using the Marsh–Dollas prevailing orientation. Quantitative phase analysis was conducted during refinement by the Rietveld method using the method of Hill and Howard.

The values of the Seebeck coefficient α and specific conductivity σ were determined by the standard technique. A sample was clamped by two copper rods and placed in an oven, where it was heated to a fixed measurement temperature. Another heater was wound on one of copper rods to create a temperature gradient ($\sim$5 K) in the sample. Measurements of temperature were carried out by two thermocouples (chromel–alumel) placed in holes drilled in the sample. Electrical conductivity was determined by measuring the voltage drop on the sample generated by an alternating-current voltage. Thus, one of the legs of each thermocouple was used as a current-carrying conductor. The Seebeck coefficient and specific electrical conductivity were determined according to the following formulas:

$$\alpha = \frac{U_{\text{e.m.f.}}}{(T_2 - T_1)}, \tag{2}$$

$$\sigma = \frac{U_{\text{et}} \cdot l}{U_{\text{sample}} \cdot R_{\text{et}} \cdot S}. \tag{3}$$

where U_{sample} is the voltage drop on the sample under AC, R_{et} is the reference resistance, S is the cross-sectional area of the sample, l is the distance between the thermocouples, $U_{\text{e.m.f.}}$ is the value of the Seebeck coefficient, and T_1 and T_2 are the temperatures of the cold and hot ends of the sample.

The thermal conductivity of the samples was determined by the radial heat flow method. To implement this method, a heater was placed along the axis of the cylindrical sample, creating a temperature gradient in the radial direction. The latter was measured by two thermocouples located along the radius. The thermal conductivity coefficient χ was calculated from the formula

$$\chi = q \ln\left(\frac{r_1}{r_2}\right) \frac{1}{2\pi(T_1 - T_2)}, \tag{4}$$

where Q is the electric power per unit heater length and T_1 and T_2 are the temperatures of the sample at distances r_1 and r_2 from the axis.

RESULTS AND DISCUSSION

A summary of the results of the x-ray phase and structural analyses is presented in Table I and Fig. 1. The typical surface structure of pressed samples, obtained using an optical microscope, is shown in Fig. 2. The observed differences, particularly in the lattice constants, are due to the different chemical compositions of the studied materials and their varying defect subsystems.

The undoped samples and those doped with antimony in the amount of 0.3 at.% Sb in lead telluride were single phase with unit cell parameter of 0.6450 nm and 0.64550 nm, respectively.

Research of PbTe containing 1 mol.% Sb_2Te_3 has not been performed, but samples containing 3 mol.% Sb_2Te_3 were characterized by an a parameter value close to that for undoped material (0.64532 nm) and by the presence of Sb_2Te_3 additional phase in the amount of 3 wt.%, which remained in the sample even after annealing. We can assume that the unit cell parameter of PbTe containing 1 mol.% Sb_2Te_3 will be close to the a value for undoped material too, while the presence of additional phases may be questioned.

$Pb_{18}Ag_1Sb_1Te_{20}$ crystallized in two phases of one structural type (NaCl) with unit cell parameter 0.64481(2) nm and 0.64334(3) nm. After pressing and annealing, one phase remained, but with higher a parameter value of 0.64509(3) nm, being however closer to the value appropriate for undoped material.

The question of the existence of two phases in $Pb_{18}Ag_1Sb_1Te_{20}$ is debatable. For better understanding of this effect, additional research is needed. We compared the XRD patterns for samples 14-15 and 14-15A and theoretically calculated ones. It was found in this case that the peaks of noncompacted and nonannealed material were much broader. This broadening is characteristic of all peaks. Therefore, the assumption of the existence of two phases with different lattice parameter was made. Good correlation was established as a result of matching the theoretical and experimental XRD patterns for these phases. Moreover, LAST-type materials are characterized by strong heterogeneity of chemical composition within the sample volume.[34] Probably, our material crystallized with significant heterogeneity, which led to the formation of the two-phase system. The components of the compounds were distributed more evenly due to diffusion processes during annealing, which caused the transition to a single-phase system.

Table I. X-ray diffraction analysis results for the synthesized materials: pressed and annealed samples

N Sample	Description of Sample	Main Phase	Content (mass%)	Unit Cell Parameter, *a* (Å)	Additional Phase, Content (mass%)	X-ray Density of Main Phase, ρ (g/cm^3)
12-1	PbTe	Structural type NaCl, space group $Fm\text{-}3m$, $Z = 4$	100	6.450	–	8.287
12-3	PbTe:Sb (0.3 at.%)		100	6.4550	–	8.268
16-1	PbTe-Sb_2Te_3 (1 at.%)					
16-2	PbTe-Sb_2Te_3 (3 at.%) (pressed and annealed)			6.4532(4)	Sb_2Te_3	8.275
14-15	$Pb_{18}Ag_1Sb_1Te_{20}$	Two phases of structural type NaCl Phase 1 (80 ± 2 mass%) a = 6.4481(2) Å Phase 2 (20 ± 1 mass%) a = 6.4334(3) Å				8.306
14-15A	$Pb_{18}Ag_1Sb_1Te_{20}$ (pressed and annealed)	Structural type NaCl, space group $Fm\text{-}3m$, $Z = 4$	100	6.4509(3)	–	8.284
14-16	$Pb_{18}Ag_2Te_{20}$		99	6.45751(19)	~1% admixture of silver telluride	8.258
14-16A	$Pb_{18}Ag_2Te_{20}$ (pressed and annealed)		99	6.4575(3)	~1% admixture of silver telluride	8.258
14-17	PbTe-Ag_2Te (10 mol.%)		~97	6.4579(3)	~3% Ag_2Te	8.257

The $Pb_{18}Ag_2Te_{20}$ and PbTe-Ag_2Te (10 mol.%) materials contain additional silver telluride phases, and their unit cell parameter was significantly higher than for pure PbTe. Here, it is necessary to consider the accuracy of the x-ray phase analysis. It is generally accepted that the accuracy of this method for determination of additional phase is ~3% to 5%. However, phases with content as low as 1% can be identified for substances having both highly symmetric lattice (cubic, tetragonal, hexagonal symmetry) and small unit cell parameters.

The results of the thermoelectric property study are presented in Fig. 3. Doping by antimony improved the electrical conductivity and thermoelectric coefficient of the material. However, probably due to growth of the electronic component, the thermal conductivity of PbTe:Sb was higher than that of pure PbTe. However, this disadvantage of material doped by antimony is compensated by a rather high value of the thermoelectric power, and consequently its dimensionless thermoelectric figure of merit far exceeds the value for pure lead telluride.

The formation of PbTe-Sb_2Te_3 solid solution predictably reduces the thermal conductivity of the base material, but the electric conductivity and Seebeck coefficient decrease simultaneously, resulting in the lowest ZT values among the studied materials. Analyzing the $ZT(T)$ curves for PbTe and PbTe-Sb_2Te_3 in the temperature range of $T > 600$ K, one can still expect improvement of the thermoelectric efficiency of solid solution compared with lead telluride.

In $Pb_{18}Ag_1Sb_1Te_{20}$ we managed to reach sufficiently high values of the Seebeck coefficient (up to 0.6 mV/K). A significant decrease in the thermal conductivity compared with pure PbTe compensates for the decrease of the material electrical conductivity, and the ZT parameter reaches values as high as those for PbTe:Sb (~1).

We find the behavior of the temperature dependence of the thermoelectric parameters of $Pb_{18}Ag_2Te_{20}$ to be most interesting. Since silver is an acceptor, replacement of antimony atoms by silver in the chemical formula $Pb_{18}Ag_1Sb_1Te_{20}$ should lead to a reduction in the specific electrical conductivity because of the decrease of the electron concentration (majority carriers). However, an increase of the σ and α values is observed experimentally. A ZT value >2 was obtained at $T = 500$ K due to the reduced thermal conductivity coefficient, which is the lowest among all the studied materials.

Further modification of the properties of lead telluride by addition of 10 mol.% Ag_2Te did not produce significant improvement in the dimensionless thermoelectric figure of merit in the temperature range from 400 K to 600 K. When low values of thermal conductivity are reached, the specific electrical conductivity of the material decreases simultaneously. As for PbTe-Sb_2Te_3 solid solutions, high ZT values can be expected in the higher tempera-

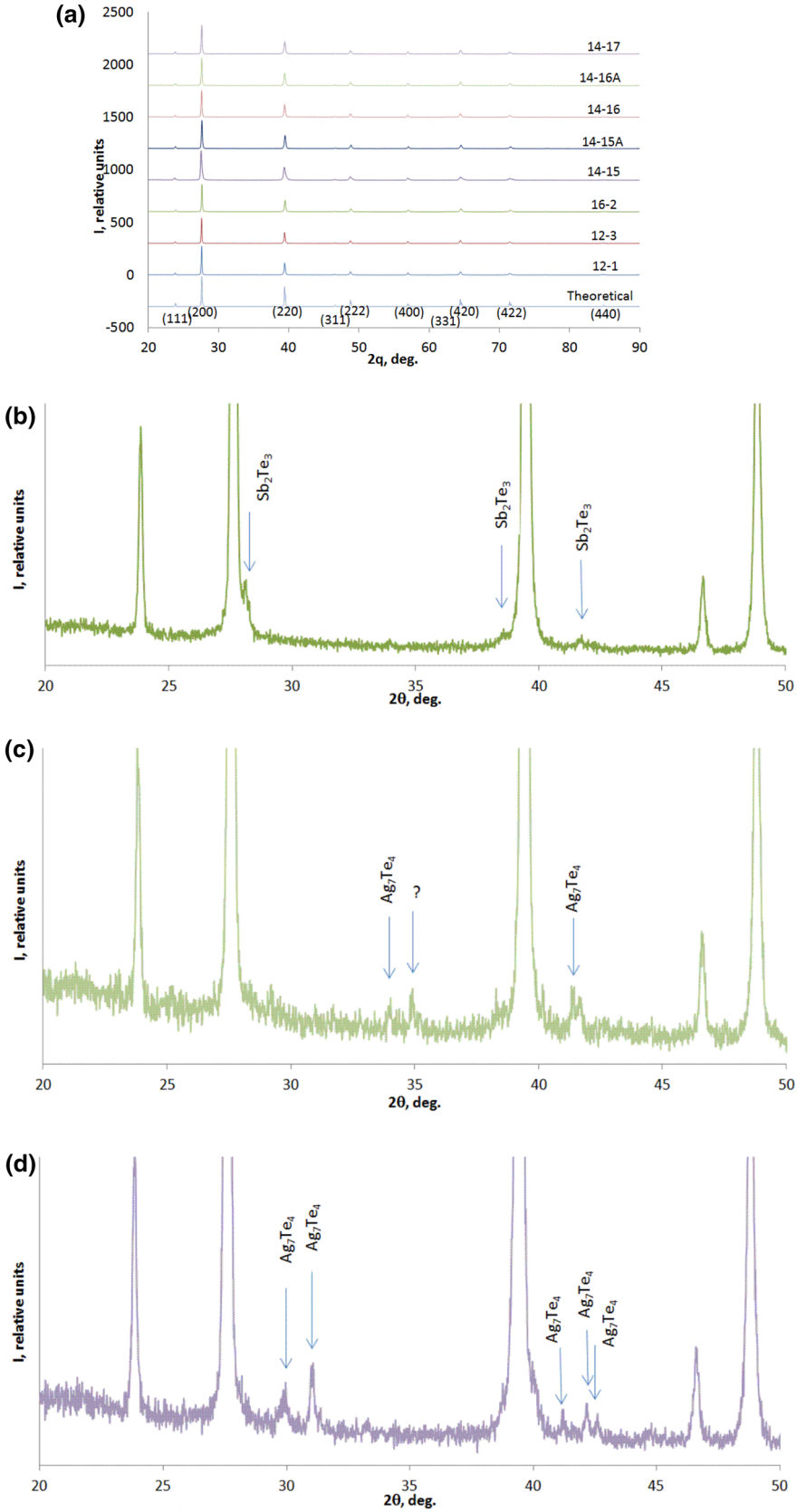

Fig. 1. XRD patterns of thermoelectric samples (a) and their fragments for samples 16-2 (b), 14-16A (c), and 14-17 (d). Peaks from additional phases are marked by arrows.

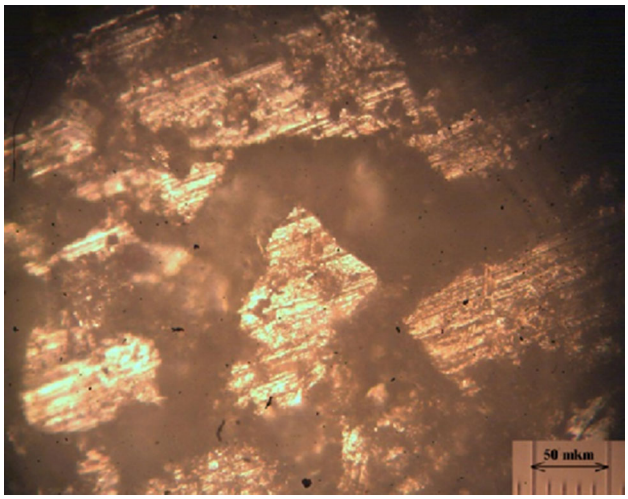

Fig. 2. Typical surface structure of pressed sample of fraction 0.05 mm to 0.5 mm.

ture range, due to the changing nature of the $\alpha(T)$ dependence at $T > 550$ K.

Some samples showed very low values of thermal conductivity, therefore detailed analysis of these results and peculiarities including the errors in the thermal conductivity measurement using the radial heat flow method is required. First of all, it should be noted that values close to our thermal conductivity values were obtained for similar materials ($Ag_{1-x}Pb_{18}BiTe_{20}$ and PbTe-Ag_2Te) in Ref. 32 [~0.5 W/(m·K)] and Ref. 33 [~0.3 W/(m·K) to 0.5 W/(m·K)]. The main disadvantage of the radial heat flow method for measurement of the thermal conductivity is the need to preserve a length-to-diameter ratio of $L/d \approx 4$ when preparing the samples and the need to drill a hole along the axis of a brittle sample. Failure to comply with these requirements and inaccuracies in measurement of the geometric dimensions, as well as thermal front disturbance in the vicinity of thermocouples can cause errors of up to ~25%.[35]

To determine the actual error, we performed a measurement of the thermal conductivity of cylindrical PTFE samples with $L/d \approx 1$, as well as thermoelectric cores. The average value of the measured thermal conductivity was 0.27 W/(m·K), versus the tabulated value of 0.25 W/(m·K). Thus, the relative error is ~10%. Considering the similarity between the thermal conductivity value of the PTFE sample and our other samples, we can assume that the errors in both cases will be in the vicinity of this value.

On the other hand, the electronic component of the thermal conductivity was also calculated for the different samples using the Wiedemann–Franz law: $k_e/\sigma = L_0T$, where the Lorenz number $L_0 = \pi^2/2(k_B/e)^2$ for a degenerate semiconductor and $L_0 = 2(k_B/e)^2$ for a nondegenerate semiconductor. The highest values of the electrical and thermal conductivity for degenerate materials were observed for PbTe:Sb, with $k_e \approx 1$ W/(m·K) at $T \approx 500$ K. Our measured value of the full thermal conductivity is $k_e \approx 4$ W/(m·K).

Among the materials studied in this work, the lowest calculated value of the full thermal conductivity is observed for $Pb_{18}Ag_2Te_{20}$, i.e., $k_e \approx 0.12$ W/(m·K) at $T \approx 500$ K. The experimentally measured value of the full thermal conductivity for this material is ~0.16 W/(m·K). It should also be noted that, for degenerate materials, the calculated values of k_e are nearly twice as low. In view of these results, we can assume that our values of the thermal conductivity obtained by the radial heat flow method are adequate.

Thus, taking into account the error estimate of ~10% for the thermal conductivity, the error of the electrical conductivity of 15%, and the 10% error for the Seebeck coefficient, the relative error for the ZT values is ~35%.

For more detailed analysis of the mechanisms of the influence of the chemical composition on the electrical properties of materials in the LAST system, research of the Hall effect at a temperature of 300 K was conducted. The results are presented in Table II. It is established that the carrier mobility in PbTe-Ag_2Te (10 mol.%) samples far exceeds that for undoped PbTe samples, but their concentration is two orders of magnitude lower, which leads to relatively low conductivity values. Taking into account that silver and excess tellurium in PbTe are acceptors, we may conclude that the observed patterns are as expected.

The question of why carrier concentration reduction is not observed for the $Pb_{18}Ag_2Te_{20}$ samples while it is observed for the $Pb_{18}Ag_1Sb_1Te_{20}$ samples is more difficult. The atoms of antimony and silver should be placed on the cationic sublattice, according to the mechanism of LAST compound formation,[15] and with the same quantity ($N_{Sb}/N_{Ag} = 1$), the electrical effect should be offset, because Sb_{Pb} is a donor and Ag_{Pb} is an acceptor. In sample 14-15A, the carrier concentration would have to be commensurate with that in pure PbTe, whereas in sample 14-16A it should be reduced. The observed patterns can be explained for the case of $Pb_{18}Ag_1Sb_1Te_{20}$ by considering the availability of intrinsic point defects of lead telluride. n-Type pure lead telluride exhibits tellurium vacancies that are donors, as shown in our previous studies.[12,13] It is very likely that atoms of antimony fill tellurium vacancies, forming acceptor defects, during LAST compound formation, as antimony is an amphoteric impurity: Sb_{Te}^{-}. Silver atoms remain uncompensated, further reducing the concentration of electrons. Moreover, addition of antimony will increase the carrier mobility via their filling of the tellurium vacancies, which effectively scatters electrons as shown in Ref. 13. This can be explained by the fact that substitution of defects leads to poor scattering of electrons in comparison with scattering at vacancies.

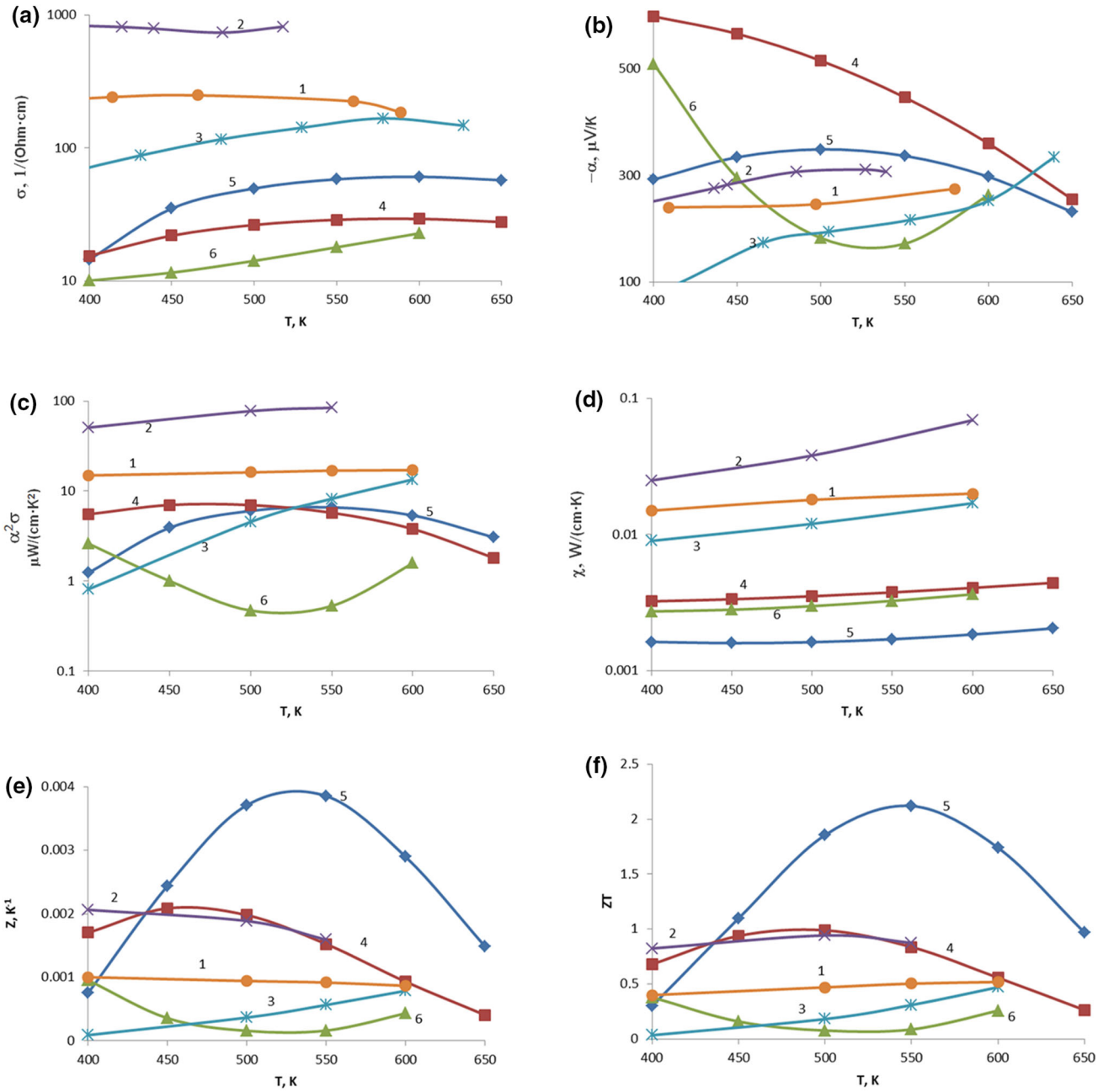

Fig. 3. Temperature dependence of specific electrical conductivity σ (a), Seebeck coefficient α (b), specific thermoelectric power $\alpha^2\sigma$ (c), coefficient of thermal conductivity χ (d), thermoelectric figure of merit Z (e), and dimensionless thermoelectric figure of merit ZT (f) for samples: PbTe (●)—1, PbTe:Sb (0.3 at.%) (×)—2, PbTe-Sb_2Te_3 (1 mol.%) (*)—3, $Pb_{18}Ag_1Sb_1Te_{20}$ (■)—4, $Pb_{18}Ag_2Te_{20}$ (◇)—5, PbTe-Ag_2Te (10 mol.%) (▲)—6.

Table II. Results of Hall research for pressed and annealed thermoelectric samples at temperature T = 300 K

Number of Sample	Content of Sample	Specific Electrical Conductivity, σ (Ω^{-1} cm^{-1})	Carrier Concentration, n (cm^{-3})	Carrier Mobility μ (cm^2 V^{-1} s^{-1})
12-1	PbTe	192.18	3.43×10^{19}	34.98
14-15A	$Pb_{18}Ag_1Sb_1Te_{20}$	6.18	3.11×10^{17}	124.23
14-16A	$Pb_{18}Ag_2Te_{20}$	57.80	1.46×10^{19}	22.58
14-17A	PbTe-Ag_2Te (10 mol.%)	19.43	4.90×10^{17}	247.75

Silver atoms show only weak acceptor properties in the case of $Pb_{18}Ag_2Te_{20}$ due to the small change of the carrier concentration. Placement of silver at anionic sites is unlikely. Therefore, we can assume that, due to the increase of the unit cell parameter compared with pure lead telluride, electroneutral complexes such as Ag_2, localized at interstitial positions, are formed. Such defects practically do not impact on the electronic subsystem of the material, but reduce its thermal conductivity. Furthermore, additional phonon scattering centers may be additional phases identified at the ~1 wt.% level. However, it is necessary to conduct additional studies on material with this chemical composition to confirm our assumptions and formulate objective conclusions.

CONCLUSIONS

1. Synthesis of materials was carried out, research samples were obtained, x-ray structural and phase analyses were conducted, and the Hall effect and temperature dependences of thermoelectric properties of PbTe, PbTe:Sb, PbTe-Sb_2Te_3, $Pb_{18}Ag_1Sb_1Te_{20}$, $Pb_{18}Ag_2Te_{20}$, and PbTe-Ag_2Te were measured.
2. It was found that the value of the dimensionless thermoelectric figure of merit is $ZT \approx 1$ for PbTe:Sb (0.3 at.%) and $Pb_{18}Ag_1Sb_1Te_{20}$ in the temperature range from 450 K to 550 K, while $ZT \approx 2$ for $Pb_{18}Ag_2Te_{20}$ in the temperature range from 500 K to 600 K. The thermoelectric capacity of the other materials in the studied temperature range is significantly lower.
3. It is shown that the high values of the thermoelectric figure of merit for PbTe:Sb were achieved through a significant increase of the conductivity of the material due to the donor action of antimony atoms, while for $Pb_{18}Ag_1Sb_1Te_{20}$ and $Pb_{18}Ag_2Te_{20}$ the high values were achieved through a reduction of the thermal conductivity, resulting from the creation of a significant number of phonon scattering centers.

ACKNOWLEDGEMENTS

This research is sponsored by NATO's Public Diplomacy Division in the framework of "Science for Peace" (NATO.NUKR.SFPP 984536).

REFERENCES

1. L.-D. Zhao, V.P. Dravid, and M.G. Kanatzidis, *Energy Environ. Sci.* (2014). doi:10.1039/C3EE43099E.
2. J.R. Sootsman, D.Y. Chung, and M.G. Kanatzidis, *Angew. Chem. Int. Ed.* 48, 8616 (2009).
3. A.V. Dmitriev and I.P. Zvyagin, *Usp. Fiz. Nauk* 180, 821 (2010).
4. H. Wang, J.-H. Bahk, C. Kang, J. Hwang, K. Kim, J. Kim, P. Burke, J.E. Bowers, A.C. Gossard, A. Shakouri, and W. Kim, *PNAS* 111, 10949 (2014).
5. T.M. Tritt, H. Böttner, and L. Chen, *MRS Bull.* 33, 366 (2008).
6. J.-C. Zheng, *Front. Phys. Chin.* 3, 269 (2008).
7. A.O. Epremyan, V.M. Arutyunyan, and A.I. Vaganyan, *Int. Sci. J. Altern. Energy Ecol.* 5, 7 (2005).
8. A.V. Shevelkov, *Russ. Chem. Rev.* 77, 1 (2008).
9. Y. Pei, A. LaLonde, S. Iwanaga, and G.J. Snyder, *Energy Environ. Sci.* (2011). doi:10.1039/C0EE00456A.
10. L.D. Borisova, *Phys. St. Sol. (a)* 53, K19 (1979).
11. C.M. Jaworski, J. Tobola, E.M. Levin, and K. Schmidt-Rohr, *J. Heremans Phys. Rev. B* (2009). doi:10.1103/PhysRevB.80.125208.
12. D.M. Freik, C.A. Kryskov, I.V. Horichok, T.S. Lyuba, O.S. Krynytsky, and O.M. Rachkovsky, *J. Thermoelectricity* 2, 42 (2013).
13. D.M. Freik, S.I. Mudryi, I.V. Gorichok, R.O. Dzumedzey, O.S. Krunutcky, and T.S. Lyuba, *Ukr. J. Phys.* 59, 706 (2014).
14. P.-W. Zhu, Y. Imai, Y. Isoda, Y. Shinohara, X.-P. Jia, and G.-T. Zou, *Chin. Phys. Lett.* 22, 2103 (2005).
15. K.-F. Hsu, S. Loo, F. Guo, W. Chen, J.S. Dyck, C. Uher, T. Hogan, E.K. Polychroniadis, and M.G. Kanatzidis, *Science* 303, 818 (2004).
16. H. Hazama, U. Mizutaniand, and R. Asahi, *Phys. Rev. B* 73, 115108 (2006).
17. E. Quarez, K.F. Hsu, R. Pcionek, N. Frangis, E.K. Polychroniadis, and M.G. Kanatzidis, *J. Am. Chem. Soc.* 127, 9177 (2005).
18. J. Sootsman, R. Pcionek, H. Kong, C. Uher, and M.G. Kanatzidis, *Mater. Res. Soc. Symp. Proc.* 886, 0886-F08-05 (2005).
19. D. Bilc, S.D. Mahanti, E. Quarez, K.F. Hsu, R. Pcionek, and M.G. Kanatzidis, *Phys. Rev. Lett.* 93, 146403-1 (2004).
20. F. Yan, T.J. Zhu, S.H. Yang, and X.B. Zhao, *Phys. Scrip.* 129, 116 (2007).
21. J.K. Lee, M.W. Oh, S.D. Park, B.S. Kim, B.K. Min, M.H. Kim, and H.W. Lee, *Electron. Mater. Lett.* 8, 659 (2012).
22. S. Perlt, Th Hoche, J. Dadda, E. Muller, P.B. Pereira, R. Hermann, M. Sarahan, E. Pippel, and R. Brydson, *J. Solid State Chem.* 193, 58 (2012).
23. J. Dadda, E. Muller, B. Klobes, P. Bauer-Pereira, and R. Hermann, *J. Electron. Mater.* 41, 2065 (2012).
24. J. Dadda, E. Müller, S. Perlt, T. Höche, P. Bauer-Pereira, and R.P. Hermann, *J. Mater. Res.* 26, 1800 (2011).
25. L. Wu, J.-C. Zheng, J. Zhou, Q. Li, J. Yang, and Y. Zhu, *J. Appl. Phys.* 105, 094317-1 (2009).
26. D. Bilc, S.D. Mahanti, E. Quarez, K.-F. Hsu, R. Pcionek, and M.G. Kanatzidis, *Phys. Rev. Lett.* (2004). doi:10.1103/PhysRevLett.93.146403.
27. K. Hoang, S.D. Mahanti, J. Androulakis, and M.G. Kanatzidis, *Mater. Res. Soc.* 886, 0886-F05-06.1 (2006).
28. K. Hoang, S.D. Mahanti, and P. Jena, *Phys. Rev. B* 76, 115432-1 (2007).
29. S.V. Barabash, V. Ozolins, and C. Wolverton, *Phys. Rev. Lett.* (2008). doi:10.1103/PhysRevLett.101.155704.
30. F. Ren, E.D. Case, E.J. Timm, and H.J. Schock, *J. Alloys Compd.* 455, 340 (2008).
31. F. Ren, E.D. Case, E.J. Timm, E. Lara-Curzio, and R.M. Trejo, *Acta Mater.* 58, 31 (2010).
32. Y. Pei, N.A. Heinz, A. LaLonde, and G.J. Snyder, *Energy Environ. Sci.* 4, 3640 (2011). doi:10.1039/C1EE01928G.
33. O. Falkenbachr, A. Schmitzz, D. Hartung, T. Dankworf, G. Koch, L. Kienlea, P.J. Klar, E. Muellerr, and S. Schlechtr, Thermoelectric Properties of Nanostructured $AgPb_mBiTe_{2+m}$ (The 2014 International Conference on Thermoelectrics, Nashville, Tennessee, USA, July 6–10, 2014) http://abstracts.its.org/abstractdetails/10552. Accessed 6 July 2014.
34. E.M. Levin, B.A. Cook, K. Ahn, M.G. Kanatzidis, and K. Schmidt-Rohr, *Phys. Rev. B* 80, 115211 (2009). doi:10.1103/PhysRevB.80.115211.
35. D.M. Freik, R.Y. Mykhajlyonka, and V.M. Klanichka, *Phys. Chem. Solid St. (Ukr.)* 5, 173 (2004).